PHYSICAL REVIEW E VOLUME 54, NUMBER 3 SEPTEMBER 1996

Shape fluctuations of droplets in emulsions

Weicheng Cai
Exxon Research and Engineering Company, Annandale, New Jersey 08801

(Received 19 July 1995; revised manuscript received 26 March 1996)

We give a statistical theory of shape fluctuations of droplets in emulsions. We have calculated the normalized mean-square displacement $\Delta\sigma$ of shape fluctuations analytically in both two and three dimensions to first order in volume fraction ϕ. We also performed computer simulations to study fluctuations in two dimensions up to high area fractions. The results at low ϕ_A are in excellent agreement with the analytical prediction. [S1063-651X(96)08709-0]

PACS number(s): 82.70.Kj

Emulsions are mixtures of two immiscible fluids, one of which is dispersed in the other. The structure of emulsions is inherently unstable against the phase separation of two immiscible fluids because of the high cost of the interfacial energy between them. However, an appropriate surfactant that adsorbs on the interface of the two fluids can kinetically stabilize emulsions indefinitely. Practical uses of emulsions have been found in foods, cosmetics, pharmaceuticals, and agricultural products [1,2], and have brought about a great interest in studying their properties.

The motivation for this work is Gang, Krall, and Weitz's [3] experiments on shape fluctuations of droplets in emulsions. It is known that a liquid droplet will be spherical at zero temperature. Thermal fluctuations, however, give an extra energy of the order of k_BT, where T is the temperature and k_B the Boltzmann constant, to the liquid droplet and deform its shape away from spherical. The degree of deformation can be characterized by the ratio of the average displacement of every element on the droplet surface to the radius of the undeformed sphere, which is proportional to the ratio of k_BT to the surface energy of the droplet. In Gang, Krall, and Weitz's experiments, the interfacial tension Γ is about 10 dyn/cm, and the radius a of the droplets is about 1 μm. At room temperature, the above-defined quantity for measuring the magnitude of shape fluctuations is of order 10^{-7}. They performed diffusing-wave spectroscopy experiments on both suspensions of effective hard spheres and emulsion droplets. They interpreted differences in the dynamic scattering spectra as due to shape fluctuations, and through use of a simple model were able to extract its small magnitude. From that, they found, surprisingly, that the shape fluctuations of droplets are strongly correlated to the volume fraction ϕ; it increases with the volume fraction, negligibly at small ϕ, and very rapidly at higher volume fractions.

The strong dependence of the droplet shape fluctuations on their volume fraction indicates that interactions among droplets are important in this problem. First, we can eliminate the hydrodynamic effects on them through the background fluid, because the properties we are concerned with are static, and hydrodynamics does not play a role. Droplet-droplet collisions, on the other hand, will contribute an extra energy source to the shape fluctuations. We take the point of view that collisions are the cause of those observed phenomena, and develop a model, attempting to make a quantitative comparison to experiments. A simple model system which we adopt for this problem consists of deformable colloidal particles, or droplets. Our aim in this paper is to calculate how translational degrees of freedom couple to the geometry of individual droplets for our model system.

We first review the shape fluctuation calculations [3] for an isolated droplet. The geometry of a droplet is specified by the radius vector $\mathbf{R}(\Omega)=R(\Omega)\hat{\mathbf{r}}$ which points from the origin to the surface element at angular position $\Omega=(\theta,\phi)$, and $\hat{\mathbf{r}}$ is the radial unit vector. The magnitude of shape fluctuations can be characterized by the normalized mean-square displacement of the droplet surface as

$$\Delta\sigma=\langle(R(\Omega)-a)^2\rangle/a^2, \tag{1}$$

where $\langle\,\rangle$ denotes the ensemble average over all different positions and shapes of droplets. a is the radius determined from the volume v_0 of droplets by $v_0=(4\pi/3)a^3$. To make this quantity dimensionless, it is divided by a^2. The surface energy for a droplet is given by $E=\Gamma A$, where A is the surface area of the droplet. To simplify the mathematical expressions, we work in spherical coordinates and denote the derivative on the surface of a droplet by

$$\nabla_\perp=\hat{\boldsymbol{\theta}}\frac{\partial}{\partial\theta}+\hat{\boldsymbol{\phi}}\frac{1}{\sin\theta}\frac{\partial}{\partial\phi}, \tag{2}$$

where $\hat{\boldsymbol{\theta}}$ and $\hat{\boldsymbol{\phi}}$ are unit vectors. The expression for A in terms of $R(\Omega)$ can be then obtained [4], and this gives E as

$$E=\Gamma\oint d\Omega R^2\sqrt{1+(\nabla_\perp R)^2/R^2}. \tag{3}$$

Let $R(\Omega)=a[1+\alpha(\Omega)]$, where α is the dimensionless amplitude of shape fluctuations, which can be expanded in terms of spherical harmonics: $\alpha=\Sigma_{lm}\alpha_{lm}Y_{lm}$. For small shape fluctuations, $\alpha\ll 1$, and we can expand E in terms of α, yielding

$$
\begin{aligned}
E&=\Gamma a^2 \oint d\Omega(1+\alpha)\sqrt{(1+\alpha)^2+(\nabla_\perp \alpha)^2}\\
&\approx \Gamma a^2 \oint d\Omega[1+2\alpha+\alpha^2+(\nabla_\perp \alpha)^2/2]\\
&=4\pi a^2\Gamma\left[1+(1/2\pi)\alpha_{00}+(1/8\pi)\sum_{lm}(l^2+l+2)|\alpha_{lm}|^2\right].
\end{aligned}
\tag{4}
$$

For a fixed droplet volume $v_0=4\pi a^3/3$,

$$
\begin{aligned}
v_0&=a^3\oint d\Omega(1+\alpha)^3\approx a^3\oint d\Omega(1+3\alpha+3\alpha^2)\\
&=(4\pi a^3/3)\left[1+(3/4\pi)\alpha_{00}+(3/4\pi)\sum_{lm}|\alpha_{lm}|^2\right],
\end{aligned}
\tag{5}
$$

and thus

$$\alpha_{00}=-\sum_{lm}|\alpha_{lm}|^2. \tag{6}$$

Substituting the above result into the equation for E, we have

$$E=4\pi a^2\Gamma+(a^2\Gamma/2)\sum_{l>1,m}(l-1)(l+2)|\alpha_{lm}|^2. \tag{7}$$

The equipartition theorem gives the mean-square fluctuations as

$$\langle|\alpha_{lm}|^2\rangle=\frac{k_BT}{\Gamma a^2}[(l-1)(l+2)]^{-1}. \tag{8}$$

The normalized mean-square displacement $\Delta\sigma$ is

$$\Delta\sigma=\sum_{l>1,m}|\alpha_{lm}|^2|Y_{lm}|^2=\sum_{l>1}\frac{1}{4\pi}\,\frac{2l+1}{(l-1)(l+2)}\,\frac{k_BT}{\Gamma a^2}. \tag{9}$$

This result can be understood by a simple dimensional analysis, as we argued in the beginning.

In a system with many droplets, the translational motion of droplets will be converted to surface energy when droplets collide. We can describe this energy by an interaction potential $V(r)$, where r is the distance between the centers of mass of two droplets. For deformable droplets, there will be a finite contact area when two droplets collide. This contact area, however, is very small, of the order of k_BT/Γ, which is $\sim 10^{-7}$ times the droplet surface area, and will be ignored in our consideration. Under this approximation, $V(r)$ is essentially a hard-core potential, which can be written down analytically as

$$V(r)=\begin{cases}0, & r>r_m\\ \infty, & r<r_m,\end{cases} \tag{10}$$

where r_m is the distance between the centers of mass of two droplets when they just touch. r_m depends on the shape of the two droplets and their relative orientation. For small shape fluctuations of two colliding droplets, an approximate analytical expression for r_m is

$$
\begin{aligned}
r_m=a\{&2+\alpha_1(\Omega_0)+\alpha_2(\Omega_0)\\
&+[\nabla_\perp\alpha_1(\Omega_0)+\nabla_\perp\alpha_2(\Omega_0)]^2/4\},
\end{aligned}
\tag{11}
$$

where Ω_0 specifies the direction of the unit vector pointing from the center of mass of one droplet to that of the other. The derivation of this is given in the Appendixes. To calculate the mean-square displacement $\Delta\sigma$, we rewrite Eq. (1) in terms of the one-body reduced probability density function $g_1[R(\Omega)]$ [5] as

$$\Delta\sigma=(1/n)\sum_{R(\Omega)}g_1[R(\Omega)][R(\Omega)-a]^2/a^2, \tag{12}$$

where n is the number density of droplets. For small volume fractions ϕ, $g_1[R(\Omega)]$ can be evaluated in terms of a Virial expansion, which is an expansion in terms of ϕ. Our calculation is evaluated to the first order in ϕ. The result is

$$g_1[R(\Omega)]=n\exp(-\Gamma_{\text{eff}}A/k_BT)/Z, \tag{13}$$

where A is the surface area of a droplet, $\Gamma_{\text{eff}}=\Gamma[1-(3/2\pi)(k_BT/\Gamma a^2)\phi]$ and $Z=\Sigma_{R(\Omega)}\exp(-\Gamma_{\text{eff}}A/k_BT)$. The derivation is given in the Appendixes. It is now straightforward to obtain an expression for $\Delta\sigma$,

$$\Delta\sigma=\Delta\sigma_0[1+(3/2\pi)(k_BT/\Gamma a^2)\phi]\quad\text{(3D)}, \tag{14}$$

where $\Delta\sigma_0$ is the mean-square displacement for a single droplet, given in Eq. (9). This result can be understood as follows. Shape fluctuations of one droplet increase when that droplet is in contact with others, and the amount of the increment should be proportional to the probability of one droplet touching other ones. Due to thermally induced shape fluctuations, droplets expand their surface boundaries. This is equivalent, on average, to droplets occupying more volume space by a layer of shells around the droplets with a thickness on the order of $k_BT/\Gamma a$. The probability of finding one droplet touching others is thus the probability that their shells overlap, which is $\propto n(k_BT/\Gamma a)(4\pi a^2)=3(k_BT/\Gamma a^2)\phi$. This provides an interpretation of the second term in Eq. (14). We also calculated $\Delta\sigma$ for two-dimensional (2D) droplets along the same lines as the 3D calculations. The result is

$$\Delta\sigma=\Delta\sigma_0[1+(1/\pi)(k_BT/\Upsilon a)\phi_A]\quad\text{(2D)}, \tag{15}$$

where Υ is the line tension of 2D droplets and ϕ_A their area fraction. Comparison of the 2D result to the 3D one indicates that the dimensionality in this problem does not qualitatively change the behavior of the ϕ dependence of $\Delta\sigma$. This is an important point that motivates our 2D Monte Carlo computer simulations, which will be discussed below.

Applying Eq. (14) to Gang, Krall, and Weitz's experiments, we find that the ϕ dependence of $\Delta\sigma$ is very weak at small ϕ,

$$\Delta\sigma=\Delta\sigma_0(1+2\times10^{-7}\phi). \tag{16}$$

This evidently predicts fluctuation enhancements that in practice would not be experimentally observable over the range of its validity, $\phi\rightarrow 0$. Indeed in Ref. [3], for $\phi<0.2$, the several points given display a negligible enhancement, and include 0 within error bars. At high volume fractions in

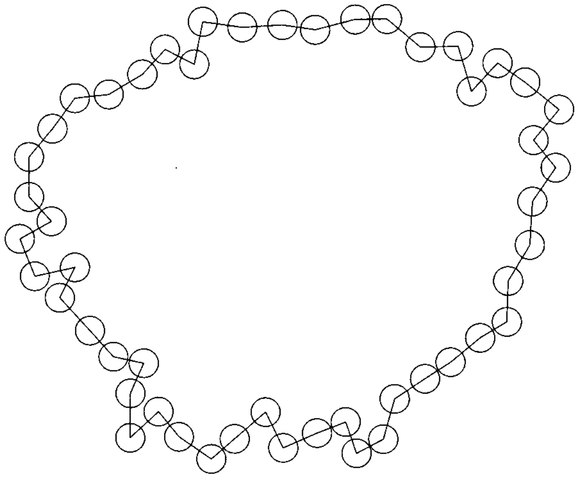

FIG. 1. A single droplet simulated by 50 neighbor-connected beads.

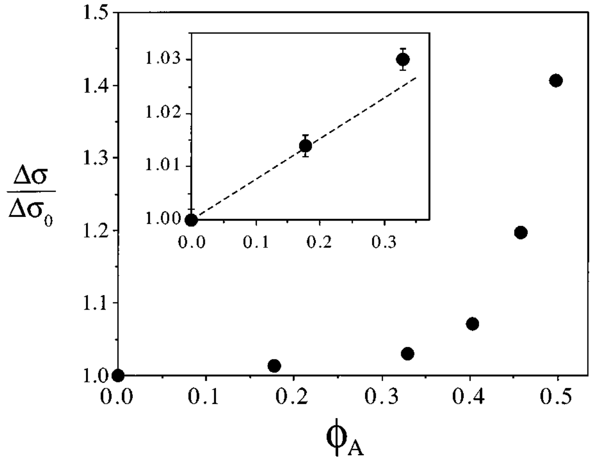

FIG. 2. Plot of $\Delta\sigma/\Delta\sigma_0$ vs ϕ_A from simulations in two dimensions. The inset includes the first three points of the plot. The dashed line is the result from analytic calculations to first order in ϕ_A.

the experiments, significant enhancements are found, with $\Delta\sigma/\Delta\sigma_0 \sim 1.8$ at $\phi \sim 0.55$. To make quantitative predictions at high volume fractions requires a calculation to higher order in ϕ than the first order one done here. Unfortunately, this calculation turns out to be very difficult mathematically. In order to proceed, we decided to perform Monte Carlo computer simulations, which allow us to determine $\Delta\sigma$ at high volume fractions. Our simulations will be restricted only to the case of 2D droplets because of limitations of real computer time. The similarity between the above 2D and 3D results, Eqs. (14) and (15), suggests that 2D simulations should predict the qualitative behavior of 3D droplets for $\Delta\sigma$ on ϕ.

In simulations, we need a mechanism to prevent droplets from interpenetrating when they move. A model solution to this problem was put forth by Leibler, Singh, and Fisher [6], which we will follow, is to construct individual droplets using a large number of neighbor-connected beads, illustrated in Fig. 1. The distance between neighboring beads within a droplet needs to be controlled to be less than a value s_0, so that, for every step of moving beads during simulations, beads from other droplets cannot penetrate it. We chose s_0 to be one and a half times the diameter d of the beads in our simulations. A line tension of droplets arises from the installation of a spring between two neighboring beads within a droplet. We used the finite extensible nonlinear elastic spring potential [7]

$$V_{\text{spring}} = \frac{k}{1-(s/s_0)^2} \quad (s < s_0 = 1.5d), \tag{17}$$

where k is the spring constant, and s the distance between two neighboring beads. The spring constant k is like the line tension Υ. Note that the spring length is measured in units of the bead diameter d, and k is thus related to Υ by $k/d^2 = \Upsilon/a$. In simulations, fixing areas of droplets is difficult to implement. We therefore changed the statistical ensemble from an area-fixed to a pressure-fixed ensemble. The pressure here is like a Lagrange multiplier, and it actually represents the pressure difference ΔP between the inside and the outside of droplets. The Gibbs potential for a system containing a number of N droplets is given by [8]

$$F = \sum_{j=1}^{N} \sum_{i=1}^{M} \frac{k}{1-(s_j^i/s_0)^2} - \sum_{j=1}^{N} \Delta P A_j, \tag{18}$$

where s_j^i is the length of ith spring in droplet j, and A_j is the area of droplet j. M is the number of beads in a droplet. We selected $M = 50$ beads for a droplet and $N = 81$ droplets bounded by periodical boundaries in a system. In the pressure-fixed ensemble, the radius of every droplet is not fixed, and its average value is determined by $k/\Delta P$. We chose $\Delta P d^2 = k$. The dimensionless quantity $k_B T/\Delta P a^2$ or $k_B T/k$ is like $k_B T/\Upsilon a$ in that it characterizes the magnitude of shape fluctuations of droplets. At small volume fractions, the ϕ dependence of $\Delta\sigma$ is very weak, as seen from the result of the analytical calculations, and is much smaller than the statistical error produced in simulations at reasonable computer time. To test the theoretical predictions, we need to increase $k_B T/k$ or $k_B T/\Delta P a^2$, which is equivalent to increasing the temperature or reducing the line tension for a real system. We set $k_B T/\Delta P d^2 = 10$. The average radius a is about $6.5d$ and, thus, $k_B T/\Delta P a^2 \sim 0.24$.

Simulations [9] were carried out by randomly moving the centers of mass of droplets and randomly varying their shapes. First, we randomly selected a droplet and moved its center of mass; in addition, we randomly chose a bead in this droplet and changed its position. The latter step was repeated 50 times in order to give every bead in the droplet an equally probable chance to move one time. Second, we repeated the above procedure 81 times to complete a simulation cycle, and then continued the process of these cycles until the system reached thermal equilibrium [9]. Finally, we performed

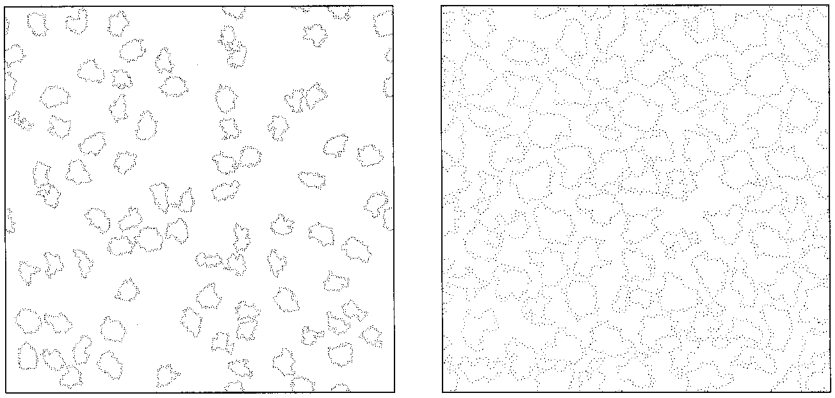

FIG. 3. Configurations of simulated droplets at two different area fractions, the left one at $\phi_A = 0.177$ and the right one at $\phi_A = 0.458$.

an ensemble average over a million cycles. $\Delta\sigma$ was calculated by the following formula:

$$\Delta\sigma = \left\langle \sum_{i=1}^{N} (1/N)(R_i - R_0)^2 \right\rangle / a^2, \tag{19}$$

where $R_0 = (1/N)\Sigma_{i=1}^{N} R_i$ and $a = \langle R_0 \rangle$. The simulation results are summarized in the plot of $\Delta\sigma/\Delta\sigma_0$ vs ϕ_A, shown in Fig. 2. At small area fractions, plotted in the inset, the simulation results are compared to the analytic predictions to first order in ϕ_A, Eq. (15). Excellent quantitative agreement is found. At higher area fractions, $\phi_A > 0.35$, large deviations from Eq. (15) are seen, and $\Delta\sigma$ develops a much stronger dependence on ϕ_A. We can understand this as follows. At low area fractions, collisions mostly occur between two droplets. But at high area fractions, multiple collisions among droplets are more likely to take place. In Fig. 3, we present snapshots of the simulated emulsion systems for two different area fractions. One is at $\phi_A = 0.177$, a low area fraction and the other is at $\phi_A = 0.458$, a relatively high area fraction. It can be noticed that at the low area fraction most of the droplets are isolated, and only a few of them are in contact. At the higher area fraction, many droplets are surrounded by others, and there are more touching droplets. Note that our simulations have not reached a very high area fraction, when compared to the limit of random close packing which is 0.82 for 2D hard disks [10]. In the experiments [3], on the other hand, the highest volume fraction is ~ 0.55, not far below the limit of random close packing for 3D hard spheres which is 0.64 [10]. It will be interesting to know if simulations at very high area fractions, close to the limit of random close packing, can predict a large increase of $\Delta\sigma$ with respect to that at low area fractions of the same magnitude as seen in the experiments. We will leave this for a future work.

In conclusion, we established a statistical model to describe the shape fluctuations of droplets in emulsions. At small volume fractions, we obtained an analytic expression for the normalized mean-square displacement $\Delta\sigma$ in both two and three dimensions. At higher volume fractions, our 2D Monte Carlo computer simulations indicate that $\Delta\sigma$ tends to increase greatly, also as seen in the experiments.

The author would like to thank his advisor, Tom Lubensky, for useful discussions, and for the suggestion to start the computer simulation. He also wants to thank Dave Weitz, Hu Gang, and Al Krall for discussions of their experiments. Finally, he thanks Gary Grest for his advice on computer simulations, and Phil Segrè for a careful reading of the manuscript. The author is grateful for financial support under NSF Grant No. 9122645.

APPENDIX A

In this appendix, we derive Eq. (11). The shapes of two droplets are specified by the radius vectors $\mathbf{R}_1(\Omega)$ and $\mathbf{R}_2(\Omega)$, respectively. $\alpha_1(\Omega)$ and $\alpha_2(\Omega)$ are introduced, as before, as dimensionless amplitudes of shape fluctuations. We designate $\mathbf{R}_0$ as the vector pointing from the center of mass of droplet 1 to that of droplet 2, which determine the relative position of the two droplets. We now need to determine how r_m depends on α_1 and α_2, and the angular position $\Omega_0 = (\theta_0, \phi_0)$ of $\mathbf{R}_0$.

A simple mathematical scheme to determine r_m is that we suppose two droplets could fictitiously intersect. The intersection will decrease when we move the two droplets away along the vector $\mathbf{R}_0$, and it eventually converges to one point when they just touch. This is illustrated in Fig. 4. The element of the intersection on both surfaces of the two droplets is determined by the angular displacement from $\mathbf{R}_0$, $\Delta\Omega_1 = (\Delta\theta_1, \Delta\phi_1)$, if measured at the center of mass of droplet 1 or $\Delta\Omega_2 = (\Delta\theta_2, \Delta\phi_2)$ if measured at that of droplet 2. $\Delta\Omega_1$ and $\Delta\Omega_2$ satisfy

$$\mathbf{R}_1(\Omega_0 + \Delta\Omega_1) - \mathbf{R}_2(\Omega_0 + \Delta\Omega_2) = \mathbf{R}_0. \tag{A1}$$

For small shape fluctuations, α_1 and α_2 are small. For a small region of intersection of two droplets, $\Delta\Omega_1$ and $\Delta\Omega_2$ are small too. We can thus expand $\mathbf{R}_1$ and $\mathbf{R}_2$ in terms of these small variables. To make the following mathematic formulas compact, we define

$$\Delta\boldsymbol{\theta}_1 = \Delta\theta_1 \hat{\boldsymbol{\theta}}_0 + \Delta\phi_1 \sin\theta_0 \hat{\boldsymbol{\phi}}_0 \tag{A2}$$

and

$$\Delta\boldsymbol{\theta}_2 = \Delta\theta_2 \hat{\boldsymbol{\theta}}_0 + \Delta\phi_2 \sin\theta_0 \hat{\boldsymbol{\phi}}_0, \tag{A3}$$

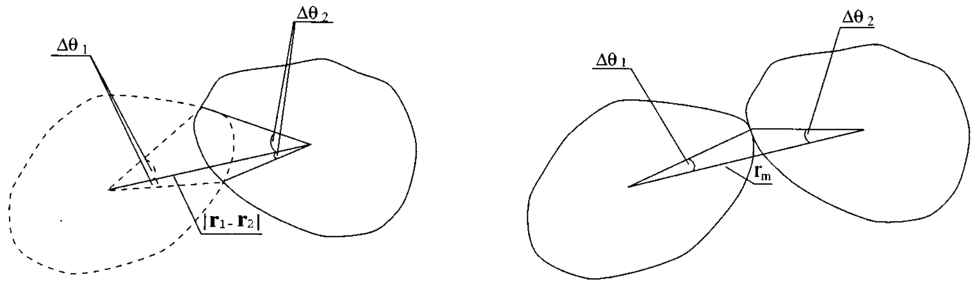

FIG. 4. The left diagram represents two intersecting droplets, and the right one two droplets that are only in contact at one surface point.

where $\hat{\boldsymbol{\theta}}_0$ and $\hat{\boldsymbol{\phi}}_0$ are the two unit vector at angular position $\Omega_0=(\theta_0,\phi_0)$ in spherical coordinates. First,

$$\hat{\mathbf{r}}_1(\Omega_0+\Delta\Omega_1)=[1-\tfrac{1}{2}(\Delta\boldsymbol{\theta}_1)^2]\hat{\mathbf{r}}_0+\Delta\boldsymbol{\theta}_1 \tag{A4}$$

and

$$\hat{\mathbf{r}}_2(\Omega_0+\Delta\Omega_2)=[1-\tfrac{1}{2}(\Delta\boldsymbol{\theta}_2)^2]\hat{\mathbf{r}}_0+\Delta\boldsymbol{\theta}_2, \tag{A5}$$

where $\hat{\mathbf{r}}_1$, $\hat{\mathbf{r}}_2$, and $\hat{\mathbf{r}}_0$ are the unit vectors along $\mathbf{R}_1$, $\mathbf{R}_2$, and $\mathbf{R}_0$, respectively. We then obtain

$$\begin{aligned}&\mathbf{R}_1(\Omega_0+\Delta\Omega_1)-\mathbf{R}_2(\Omega_0+\Delta\Omega_2)\\&\quad=a[2+\alpha_1(\Omega_0)+\alpha_2(\Omega_0)\\&\qquad-(\Delta\boldsymbol{\theta}_1^2+\Delta\boldsymbol{\theta}_2^2)/2+\Delta\boldsymbol{\theta}_1\cdot\boldsymbol{\nabla}_\perp\alpha_1(\Omega_0)\\&\qquad+\Delta\boldsymbol{\theta}_2\cdot\boldsymbol{\nabla}_\perp\alpha_2(\Omega_0)]\hat{\mathbf{r}}_0+a(\Delta\boldsymbol{\theta}_1-\Delta\boldsymbol{\theta}_2).\end{aligned} \tag{A6}$$

From Eqs. (A1) and (A6), it is evident that $\Delta\boldsymbol{\theta}_1=\Delta\boldsymbol{\theta}_2$, and this gives us

$$\begin{aligned}&|\mathbf{R}_1(\Omega_0+\Delta\Omega_1)-\mathbf{R}_2(\Omega_0+\Delta\Omega_2)|\\&\quad=a\{[2+\alpha_1(\Omega_0)+\alpha_2(\Omega_0)-\Delta\boldsymbol{\theta}_1^2\\&\qquad+\Delta\boldsymbol{\theta}_1\cdot[\boldsymbol{\nabla}_\perp\alpha_1(\Omega_0)+\boldsymbol{\nabla}_\perp\alpha_2(\Omega_0)]\}.\end{aligned} \tag{A7}$$

The right-hand sides of Eq. (A7) approaches maximum when two droplets move away and tend to touch just by one point. r_m is that maximum which is

$$\begin{aligned}r_m=a\{&2+\alpha_1(\Omega_0)+\alpha_2(\Omega_0)\\&+[\boldsymbol{\nabla}_\perp\alpha_1(\Omega_0)+\boldsymbol{\nabla}_\perp\alpha_2(\Omega_0)]^2/4\}.\end{aligned} \tag{A8}$$

APPENDIX B

In this appendix, we derive $g_1[\alpha(\Omega)]$. The free energy for a system containing N droplets is given by

$$F=\Gamma\sum_{i=1}^{N}A_i+\sum_{i<j}V(|\mathbf{r}_i-\mathbf{r}_j|), \tag{B1}$$

where A_i is the surface area for droplet i, and $\mathbf{r}_i$ and $\mathbf{r}_j$ are the position vectors pointing to the centers of mass of droplets i and j, respectively. For the grand canonical ensemble, the partition function is

$$\Xi=\sum_{p=0}^{\infty}\frac{1}{p!}x^p\int d^{3p}\mathbf{r}[D^p\alpha]e^{-\beta F}, \tag{B2}$$

where $x=e^{\beta\mu}/\lambda_T^3$ and $\beta=(k_BT)^{-1}$. Here μ is the chemical potential for the droplets in the system, and λ_T is the thermal wavelength. The one-body reduced probability density function $g_1[\alpha(\Omega)]$ is defined as [5]

$$g_1[\alpha(\Omega)]=\frac{1}{\Xi}\sum_{p=1}^{\infty}\frac{1}{(p-1)!}x^p\int d^{3(p-1)}\mathbf{r}[D^{p-1}\alpha]e^{-\beta F}. \tag{B3}$$

For a low volume fraction, the number density of droplets n is small and so is x. We can expand g_1 in powers of x,

$$g_1=xe^{-\beta\Gamma A}+Z_0x^2e^{-\beta\Gamma A}b_2[\alpha]+\cdots, \tag{B4}$$

where

$$\begin{aligned}b_2[\alpha]=(1/Z_0)&\int[D\alpha']e^{-\beta\Gamma A'}\\&\times\int d^3\mathbf{r}'\{\exp[-\beta V(|\mathbf{r}-\mathbf{r}'|)]-1\}\end{aligned} \tag{B5}$$

and $Z_0=\int[D\alpha]\exp(-\beta\Gamma A)$. x is determined by n through

$$n=\frac{k_BT}{V}\frac{\partial\ln\Xi}{\partial\mu}=Z_0x+(Z_0x)^2B_2+\cdots, \tag{B6}$$

where V is the total volume of the system, and

$$B_2=(1/Z_0)\int[D\alpha]b_2[\alpha]e^{-\beta\Gamma A}\equiv\langle b_2[\alpha]\rangle_{\text{shape}}. \tag{B7}$$

Equation (33) can be solved order by order in terms of n, and this gives

$$x=(1/Z_0)(n-B_2n^2+\cdots). \tag{B8}$$

Substituting Eq. (35) into Eq. (31), we obtain

$$g_1=n(e^{-\beta\Gamma A}/Z_0)[1+(b_2[\alpha]-B_2)n+\cdots]. \tag{B9}$$

Now we need to evaluate $b_2[\alpha]$ and $B2$:

$$\begin{aligned}b_2&=(1/Z_0)\int[D\alpha']e^{-\beta\Gamma A'}\oint d\Omega_0\int_0^{r_m}drr^2=(1/Z_0)\int[D\alpha']e^{-\beta\Gamma A'}\oint d\Omega_0(8a^3/3)[1+(\alpha+\alpha')/2\\&\quad+(\nabla_\perp\alpha+\nabla_\perp\alpha')^2/8]^3\\&\approx(2v_0/\pi)\left\{\oint d\Omega_0[1+3\alpha/2+3\alpha^2/4+3(\nabla_\perp\alpha)^2/8]+\oint d\Omega_0\langle 3\alpha/2+3\alpha^2/4+3(\nabla_\perp\alpha)^2/8\rangle_{\rm shape}\right\},\end{aligned}\tag{B10}$$

where $v_0=4\pi a^3/3$. The area A of a droplet is given by

$$A=a^2\oint d\Omega(1+\alpha)\sqrt{(1+\alpha)^2+(\nabla_\perp\alpha)^2}\approx a^2\oint d\Omega[1+2\alpha+\alpha^2+(\nabla_\perp\alpha)^2/2].\tag{B11}$$

With the aid of Eqs. (B7), (B10), and (B11), b_2-B_2 is obtained:

$$\begin{aligned}b_2-B_2&=(3v_0/2\pi)\left\{\int d\Omega_0[2\alpha+\alpha^2+(\nabla_\perp\alpha)^2/2]\right.\\&\quad\left.-\int d\Omega_0\langle 2\alpha+\alpha^2+(\nabla_\perp\alpha)^2/2\rangle_{\rm shape}\right\}=(3v_0/2\pi a^2)(A-\langle A\rangle_{\rm shape}).\end{aligned}\tag{B12}$$

Substituting the above result into Eq. (B9), we finally obtain

$$g_1=n(e^{-\beta\Gamma A}/Z_0)[1+(A-\langle A\rangle_{\rm shape})(3v_0/2\pi a^2)n+\cdots]\approx n\exp(-\beta\Gamma_{\rm eff}A)/Z,\tag{B13}$$

where $\Gamma_{\rm eff}=\Gamma[1-(3/2\pi)(k_BT/\Gamma a^2)\phi]$ and $Z=\int[D\alpha]\exp(-\beta\Gamma_{\rm eff}A)$.

[1] P. Becher, *Emulsion: Theory and Practice* (Reinhold, New York, 1965).

[2] L. L. Schramm, *Emulsions: Fundamentals and Applications in the Petroleum Industry* (ACS, Washington, D.C., 1992).

[3] Hu Gang, A. H. Krall, and D. A. Weitz, Phys. Rev. Lett. **73**, 3435 (1994); Phys. Rev. E **52**, 6268 (1995).

[4] M. Spivak, *A Comprehensive Introduction to Differential Geometry* (Publish or Perish, Boston, 1970).

[5] L. E. Reichl, *A Modern Course in Statistical Physics* (University of Texas, Austin, 1980).

[6] S. Leibler, R. Singh, and M. E. Fisher, Phys. Rev. Lett. **59**, 1989 (1987).

[7] R. B. Bird *et al.*, *Dynamics of Polymeric Liquids* (Wiley, New York, 1977), Vols. 1 and 2.

[8] K. Huang, *Statistical Mechanics* (Wiley, New York, 1963).

[9] M. P. Allen and D. J. Tildesley, *Computer Simulation of Liquids* (Clarendon, Oxford, 1990).

[10] J. G. Berryman, Phys. Rev. A **27**, 1053 (1983).